\

Wildcat Cove Drone Survey

Final Report

by

David Wallin

Department of Environmental Science

Western Washington University

September 15, 2023

Introduction

At the request of the Whatcom County Marine Resources Commission and Larrabee State Parks, I have conducted eelgrass surveys in Wildcat Cove at Larrabee State Park to assess the impact of boat launch activities on eelgrass. Surveys were conducted using an Unoccupied Aerial System (UAS). Survey flights involved the use of a Matrice 210 UAS that carried a Micasense 10-band Dual Camera system in addition to a standard RGB camera. Flights were conducted during low tide events on July 14, 17, 31 and on August 28. The objective was to standard color imagery as well multispectral imagery that could be used to assess percent cover of eelgrass and algae and changes in cover between dates. The first flight on July 14 occurred the day before the opening of recreational crabbing season. Wildcat Cove is a very popular boat launch location at all times of year but use is particularly heavy during the recreational crabbing season.

There are two species of eelgrass present in our area: *Zostera marina* and *Zostera japonica*. *Z. marina*, the native and most abundant species, is found throughout the bay's mid to sub tidal regions. *Z. japonica*, a non-native eelgrass is found throughout upper to mid-tidal ranges. Originally from Japan, *Z. japonica* is believed to have reached North American shores as an aquatic hitchhiker in the packing materials of clam exports. Although recent work by my students was successful in separating these two species using multispectral imagery, I have not attempted to do so in this analysis. Doing so would involve a much more in-depth analysis.

Methods

UAS Flights

All flights were timed to occur at or near low tides that occurred at times of day when the sun was below ~52 degrees above the horizon. Previous UAS flights at Padilla Bay have shown that flights occurring at higher sun angles results in specular reflection off the water surface resulting in glare that makes the imagery unusable. Obtaining imagery at these lower sun angles meant that the southwest edge of the cove was in shade during the 7/14 and 7/31 flight.

Prior to each flight, I placed 30 numbered ground control panels in three transect on the exposed mudflat. Along each transect, the panels were spaced ~5 m apart and the spacing between each transect was ~15 m. Prior to the survey flight, I flew over each transect at an altitude of ~5 m and took standard RGB images of each panel. These images provided me with "virtual" ground truth data that was used to model percent cover. This process is described below.

Survey flights were conducted using the DJI Pilot app. In this app, I defined a polygon that covered the entire cove. After choosing a flight altitude and desired sidelap and frontlap between images, the app calculates the spacing between flightlines. All flights were conducted in compliance with FAA Section 107 rules. The July 14 flight was conducted at an elevation of ~60 m above ground level (AGL) and resulted in a ground resolution of ~ 4 cm. All subsequent flights were conducted an elevation of ~ 40 m AGL resulting in a ground resolution of ~ 2.5 cm.

Image Processing

Each flight resulted in several thousand images that were processed using the Agisoft Metashape software (v 1.8.4). The approximate coordinates of seven ground control points (GCPs) were located in Google Earth imagery. These GCPs consisted of the edges of large rocks that could be easily located in the imagery. These GCPs enable me to co-register imagery from all three dates to facilitate change analysis. Ideally, more precise coordinates for these GCPs would have been obtained using high resolution GPS equipment but in the interest of time, I did not do this. The approximated coordinates obtained in Google Earth seemed to be sufficient for this analysis. Image processing in Agisoft Metashape resulted in a 10-band orthomosaic image for each of the three dates. For each date, 10-band TIFF files were exported from Agisoft Metashape Two versions of these TIFFs were generated for each date; one resampled to 5 cm grid cells and another resampled to 0.5 m grid cells. This larger grid cell size matches the size of my virtual ground control plots (described below).

Using the orthomosaics, I generated a series of vegetation indices in the ENVI image processing software. Each vegetation index was generated using this equation.

$$VI = \frac{B1 - B2}{B1 + B2}$$

Variables used in this equation are presented in Table 1.

Table 1: Variable used to calculated each of the three vegetation indices used in this analysis. Indices include the Normalized Difference Vegetation Index (NDVI), Normalize Difference Red Edge (NDRE) and the Normalized Difference Index (NDI).

B1	B2	Index Name	Index to:
Near-IR	Red	NDVI	Photosynthetic rate
Near-IR	Red Edge	NDRE	Chlorophyll content
Red Edge	Red	NDI	Leaf Area Index

These vegetation index images were generated using the 10-band orthomosaics with a grid cell size of 0.5 m.

"Virtual Ground Truth Data"

"Virtual" ground truth data was obtained by importing each ground control panel image into powerpoint. A 4 by 4 grid was superimposed next to each panel and the grid size was resized to match the size of each panel (Figure 1) . The panels are 45 cm by 45 cm. Resizing the grid to match the size of the ground control panel ensures that the grid samples a consistent area on the ground. The cover type was visually assessed at the corner of each grid, resulting in data for 25 points within this 45 cm by 45 cm sample grid. Percent cover for each cover type was calculated for each location. The four cover types included included eelgrass, algae (*Ulva sp.,* mostly *Ulva intestinalis)*, bare and detritus. I did not distinguish between the two species of eelgrass. Detritus is mostly composed of dead eelgrass.

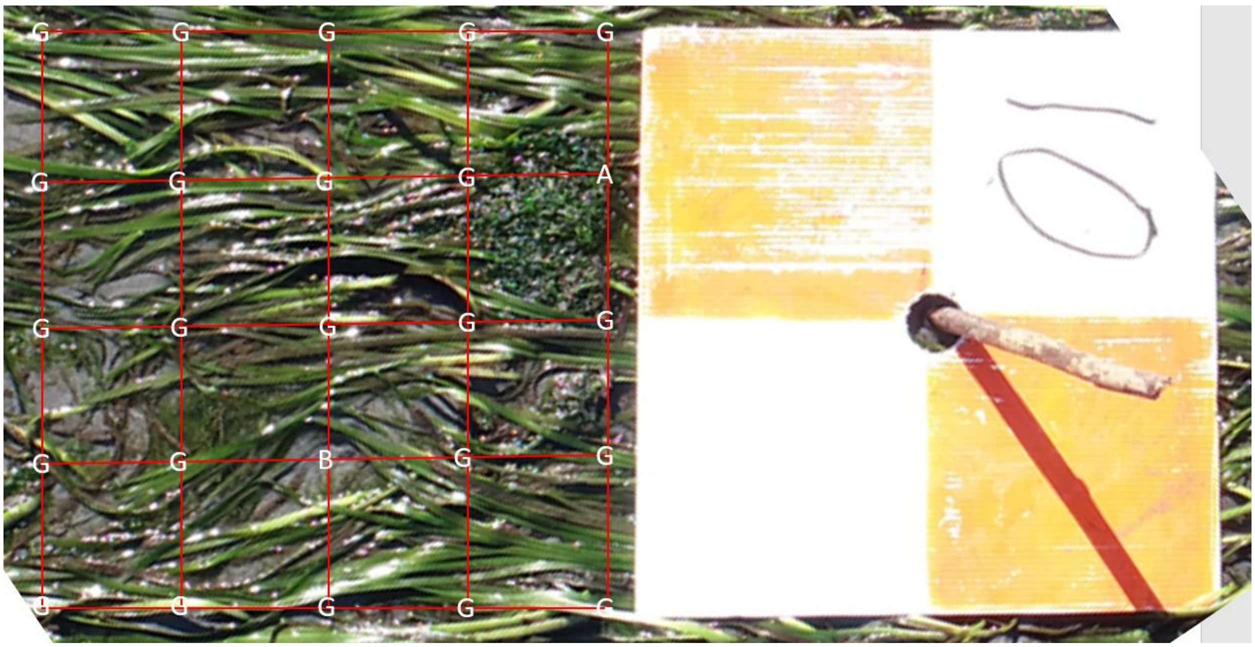

Figure 1: Example of one of the “virtual” ground control panels with 4 by 4 sample grid superimposed on the image. The cover type at the corner of each grid cell, was recorded and the percent coverage of each cover type was calculated for each of these locations. The four cover types included eelgrass (G), algae (A), bare (B) and detritus (D). Note that detritus was not present at this location.

Typically vegetation ground truth data would be obtained in the field by walking to individual points in the field and laying down a 50 cm by 50 cm sampling frame constructed from PVC tubing. This sampling frame would include a grid of string that generates 25 grid intersections identical to what is depicted in Figure 1. This ground-based sampling is quite time consuming and difficult to complete within the narrow window provided by low tide events. The use of the “virtual” ground truth data described above is faster and generates data that is equivalent to the ground-based approach.

Modelling Vegetation Cover

Although the coordinates for each of the “virtual” ground control location was not recorded, the location of each panel was quite easy to locate in the 5 cm resolution imagery. With the 5 cm resolution imagery as well as each of the three 0.5 m resolution vegetation indices loaded in ENVI, it was possible to locate a panel in the 5 cm resolution imagery, and then toggle to each of the vegetation indices to record the value for each index immediately adjacent to the panel. The data for all three dates and each index were then compiled in Excel and regression analysis was used to model vegetation cover.

Results

Color imagery

Standard color imagery for each date is presented in Figures 2-5 and enlarged subsets from each date are presented in Figure 6.

Figure 2: Color imagery for Wildcat Cove at ~10:15 on July 14, the day before the opening of crabbing season. Tide stage ~ -1.5 ft. Sun angle 45 degrees. Note denuded area through eelgrass created by boat launch activity.

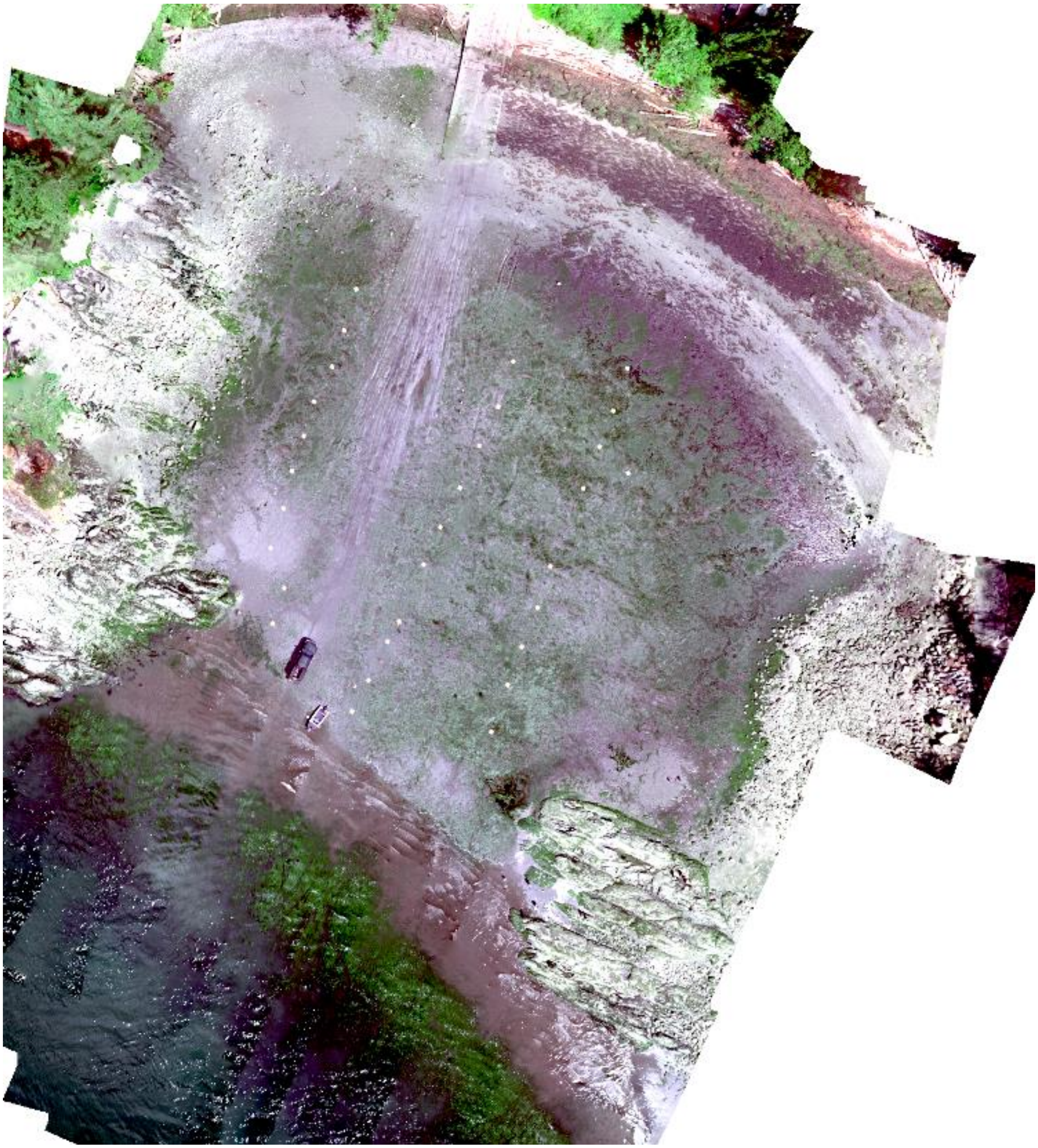

Figure 3: Color imagery for Wildcat Cove at ~noon on July 17, two days after the opening of crabbing season. Tide stage ~ -1.8 ft. Sun angle 57 degrees. Note wider denuded track through eelgrass created by boat launch activity as well as track through the subtidal eelgrass.

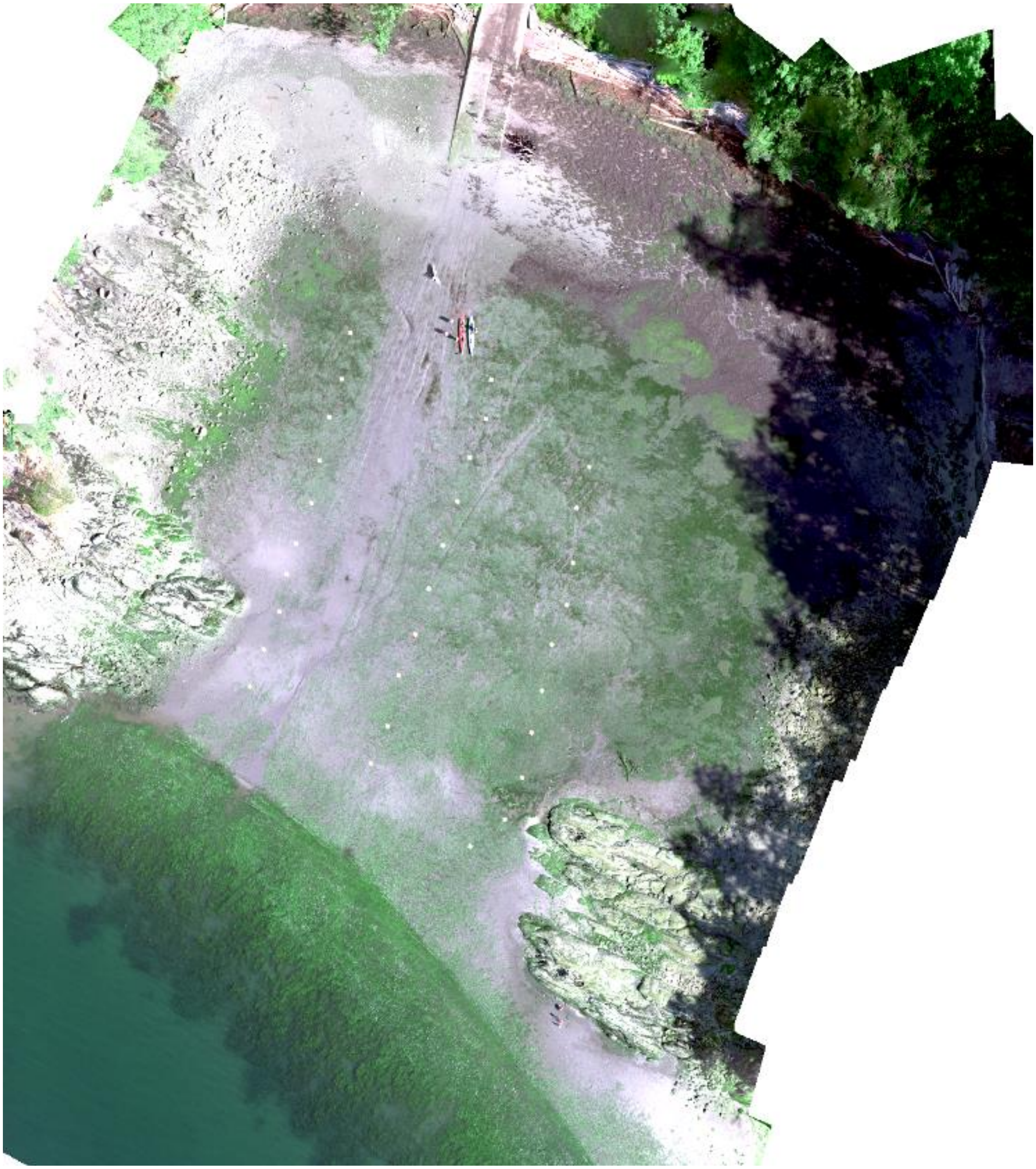

Figure 4: Color imagery for Wildcat Cove at ~10:00 on July 31. Tide stage ~ -3.1 ft. Sun angle 42 degrees. Note wider denuded track through eelgrass created by boat launch activity

Figure 5: Color imagery for Wildcat Cove at ~9:15 on August 28. Tide stage ~ -2.0 ft. Sun angle 27 degrees. Note that, as is typical for this time of year, eelgrass is beginning to senesce throughout the cove and there is a large area of dead eelgrass washed up on the upper beach (a). 100% overcast conditions on this day resulted in some glare from shallow water (b) that resulted in anomalous vegetation index values from these areas. For this reason, ground control plots from these areas were not used for modeling. Typical seasonal decline of subtidal eelgrass is also apparent (c). Denuded track through eelgrass created by boat launch activity is still present and is expanded to some degree.

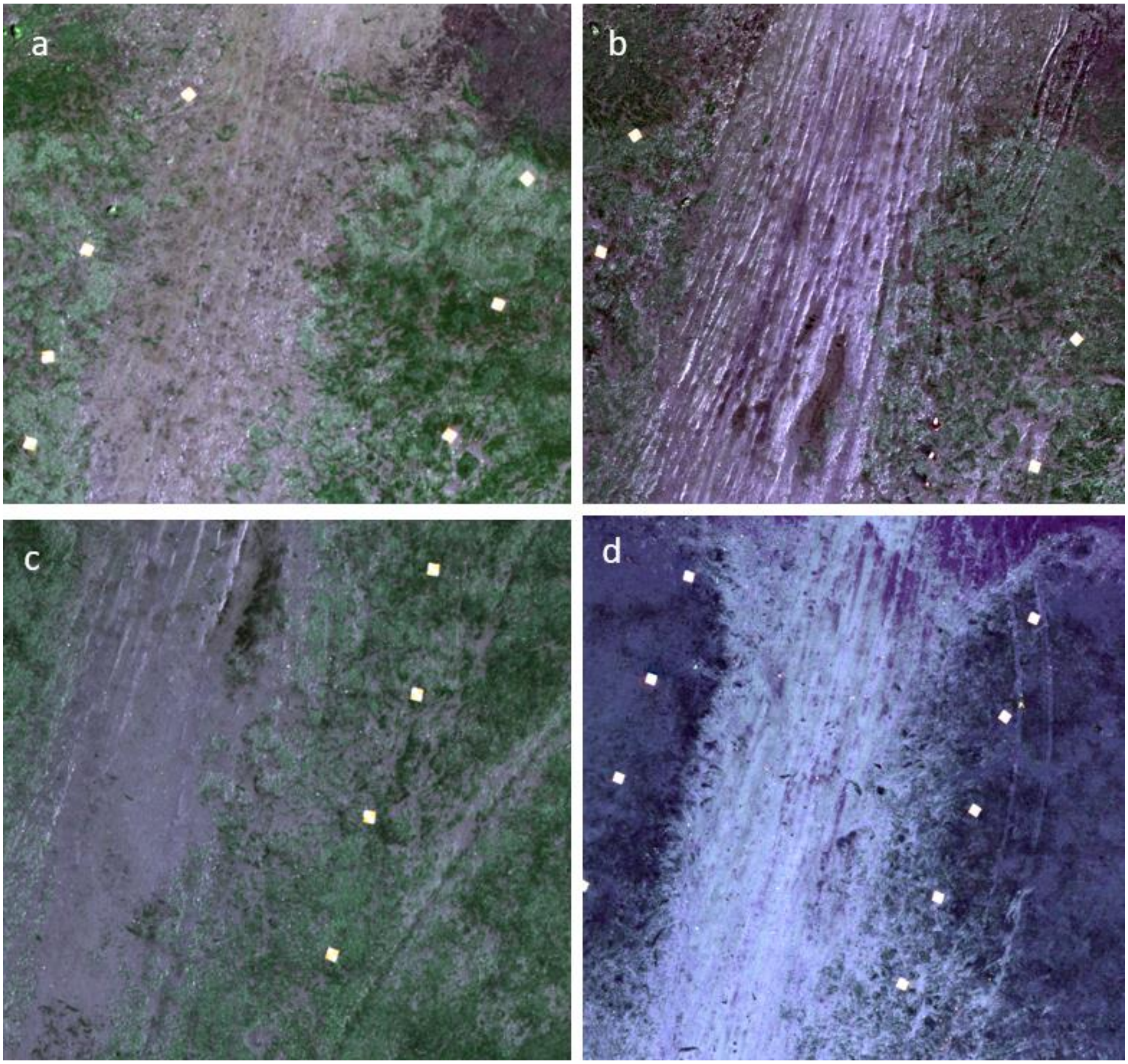

Figure 6: Details of boat launch impacts on eelgrass on (a.) July 14, (b.) July 17, (c.) July 31 and (d.) August 28

Note that a denuded track through the eelgrass on the exposed mudflat is visible on July 14 but that the width of this track has increased and more deeply rutted on July 17 after two busy days of boat launch activity on the first weekend of crabbing season. A track of reduced eelgrass cover is also visible in the subtidal eelgrass on July 14 and 17. Additional reduction of eelgrass cover and widening of the track is apparent on July 31 and August 28. Much of the decline in vegetation cover elsewhere in the cove on August 28 is simply due to typical seasonal declines.

Data from the virtual ground truth plots reveals that eelgrass is the dominant cover type in these plots during July, but by late August, senescence of eelgrass is occurring and detritus, mostly consisting of dead eelgrass, is the dominant cover type in the plots (Table 2)

Table 2: Percent cover of each cover type in the virtual ground truth plots for each date. Values are mean (Standard error).

Date	Eelgrass	Algae	Bare	Detritus	N
July 14	39.5 (5.17)	25.9 (4.29)	27.9 (4.28)	6.5 (1.46)	34
July 17	38.7 (5.00)	14.4 (4.37)	38.5 (4.96)	8.4 (1.90)	27
July 31	41.8 (4.92)	15.5 (3.62)	28.8 (4.81)	12.8 (2.10)	34
August 28	27.7 (4.80)	19.3 (5.42)	20.1 (5.52)	35.6 (5.18)	30

Note that these plots were not randomly located so variation in values between dates should not be interpreted as an unbiased estimate of temporal change in coverage.

Modeling Vegetation Cover

Data for all four dates was combined to develop a vegetation cover model using each of the vegetation indices. In addition to data from the virtual ground truth plots, for each date, I also collected vegetation index values for eight arbitrarily selected points in the subtidal eelgrass. Inspection of the images made it quite clear that these samples represented 100% eelgrass cover in July, but by late August, subtidal eelgrass appeared to be declining somewhat so no vegetation index values from this area were used in model building.

My best model was based on the NDI vegetation index to predict total percent cover of eelgrass and algae on the exposed mudflat and the subtidal eelgrass. This model is presented in Figure 7. As indicated in this figure, NDI explained 83.4 of the variation in total vegetation cover. A separate analysis using just percent cover of eelgrass was also significant, but the percent variance explained was only about 63% (Figure 8). This reduction in explained variance was due to the noise generated by the presence of algae.

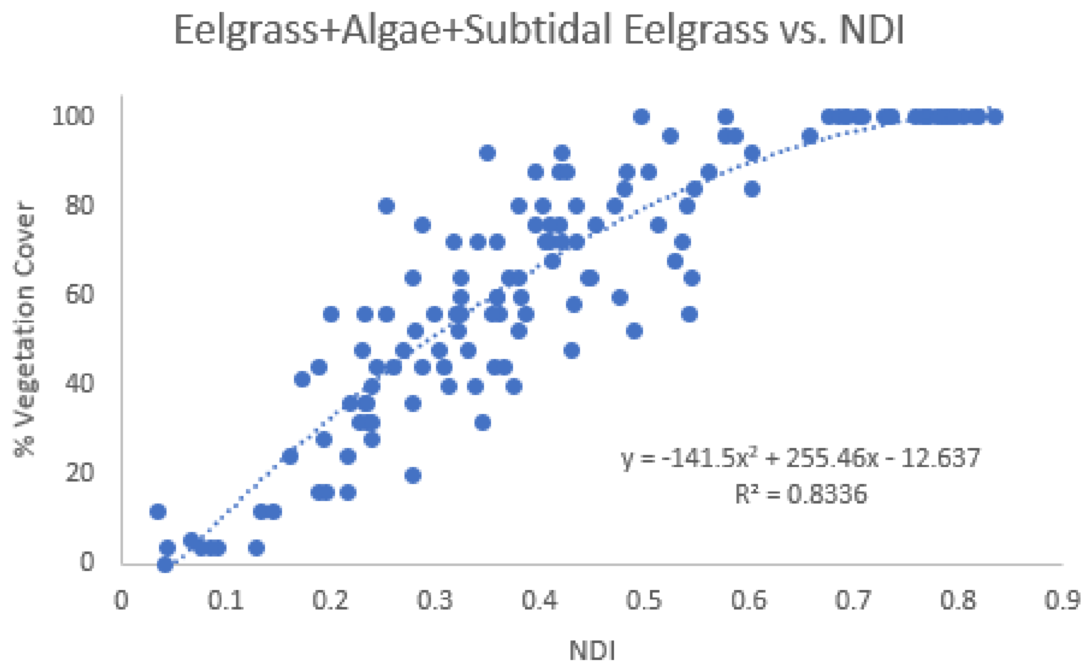

Figure 7: Percent total cover of eelgrass and algae vs. the NDI vegetation index using data from July 14, 17, 31 and August 31. N=134

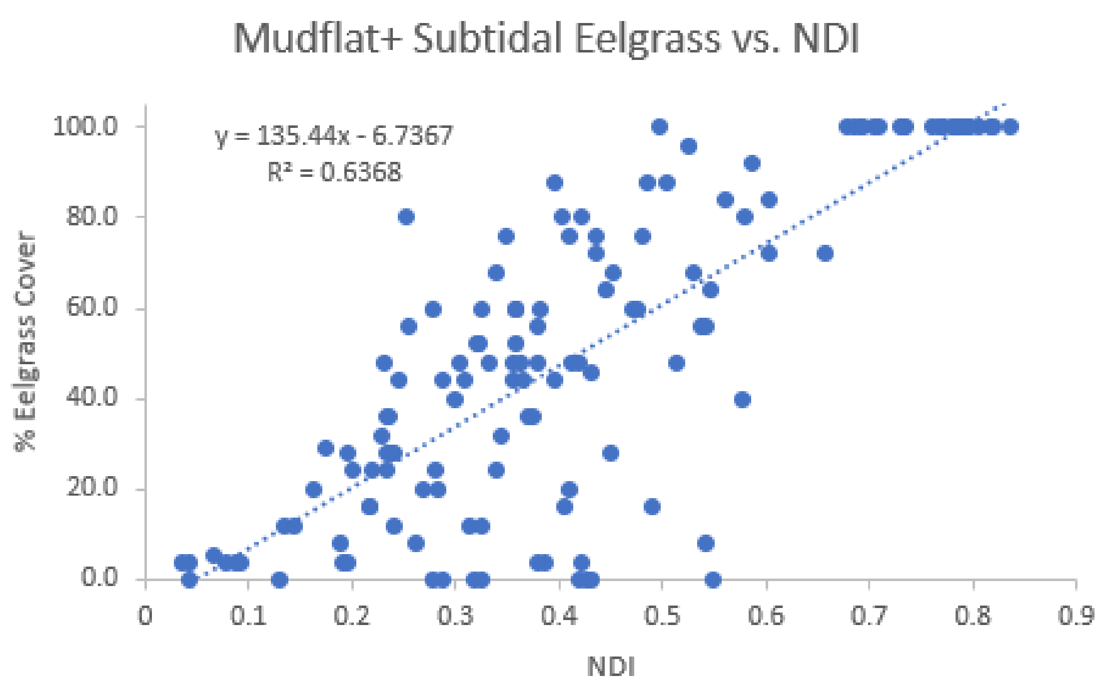

Figure 8: Percent cover of Eelgrass vs. the NDI vegetation index using data from July 14, 17, 31 and August 31. N=134. Note that lower R^2 value is due to the noise generated by the presence of algae

I then used the relationship from Figure 7 to model total vegetation cover in the study area. The model is only applied to the mudflat and area covered by the subtidal eelgrass. The results of doing so are presented in Figures 9-12.

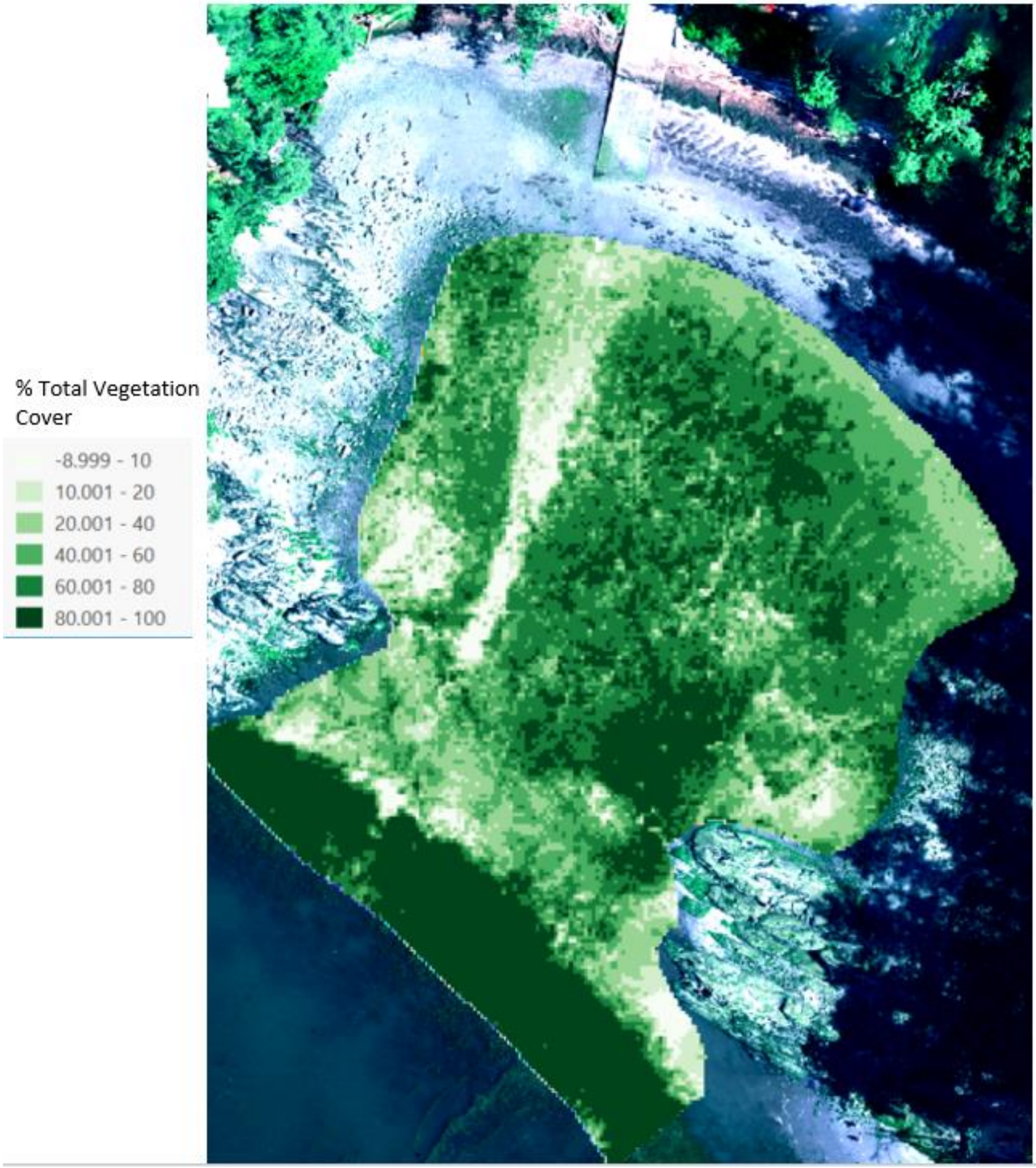

Figure 9: Percent total vegetation cover for the mudflat and subtidal eelgrass for July 14 using the NDI vegetation index and equation in Figure 7. Total vegetation cover includes both eelgrass and algae. Area outside the mudflat is the RGB image for this date to provide context relative to upland and the paved boat ramp.

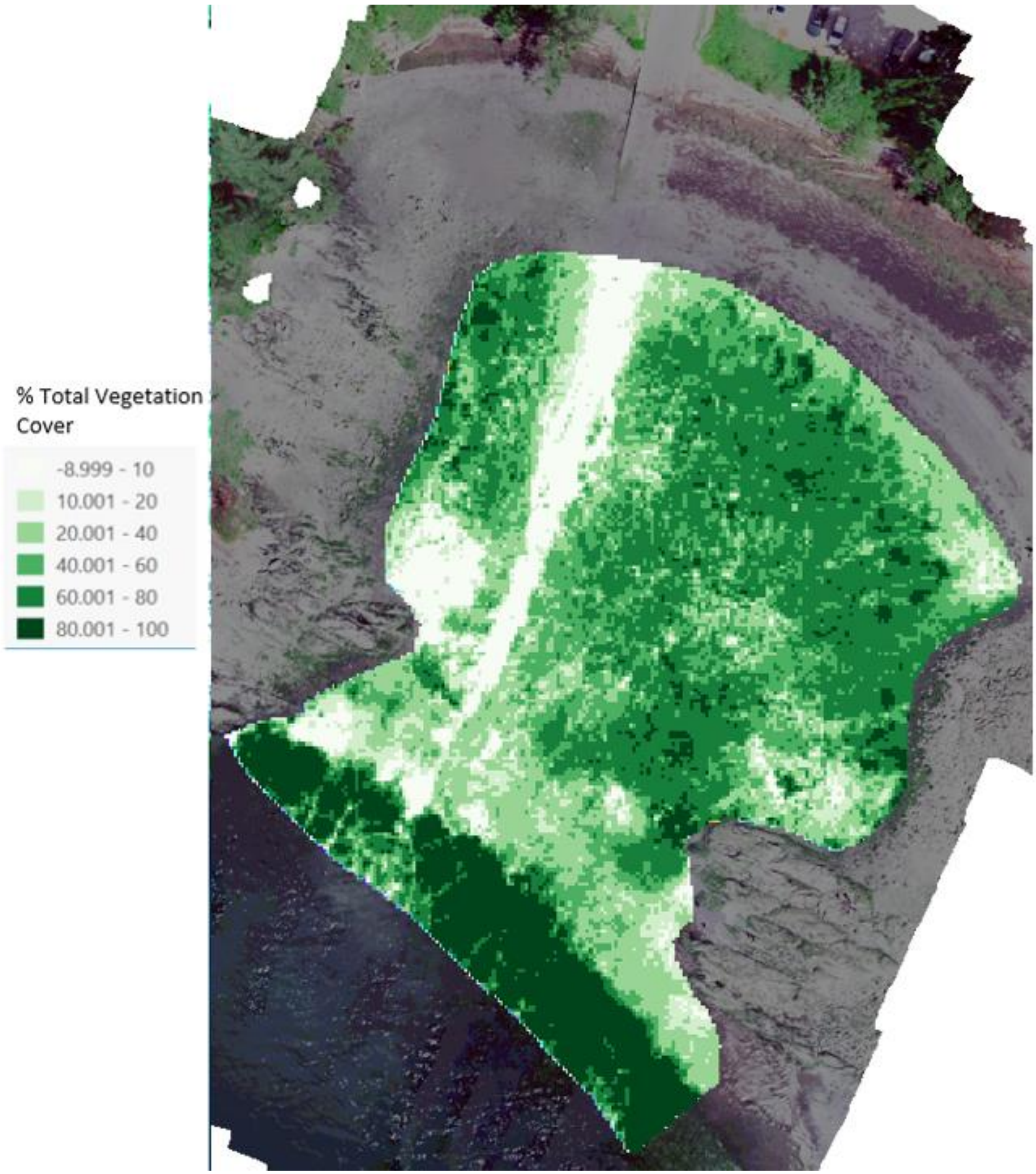

Figure 10: Percent total vegetation cover for the mudflat and subtidal eelgrass for July 17 using the NDI vegetation index and equation in Figure 7. Total vegetation cover includes both eelgrass and algae. Area outside the mudflat is the RGB image for this date to provide context relative to upland and the paved boat ramp.

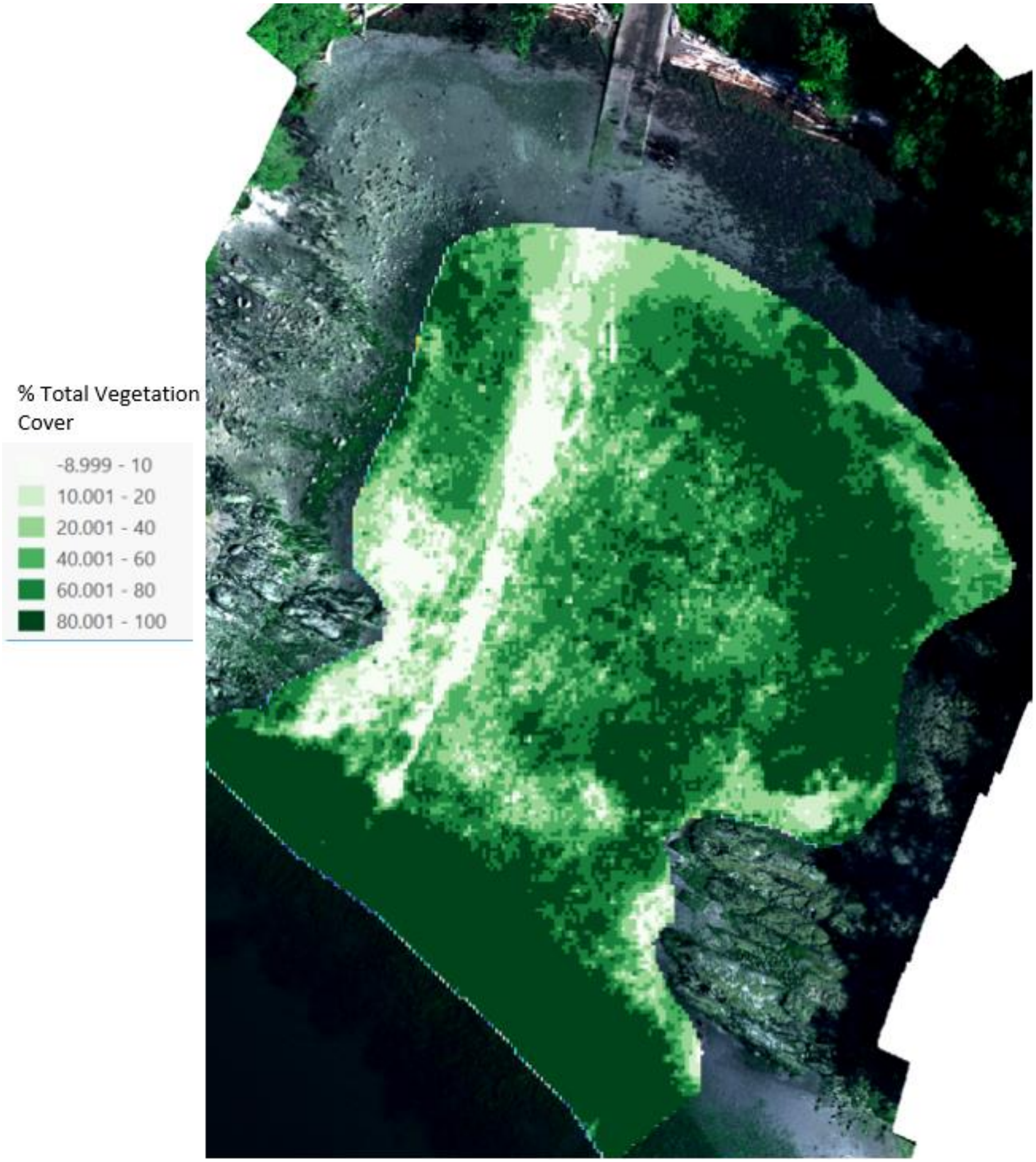

Figure 11: Percent total vegetation cover for the mudflat and subtidal eelgrass for July 31 using the NDI vegetation index and equation in Figure 7. Total vegetation cover includes both eelgrass and algae. Area outside the mudflat is the RGB image for this date to provide context relative to upland and the paved boat ramp.

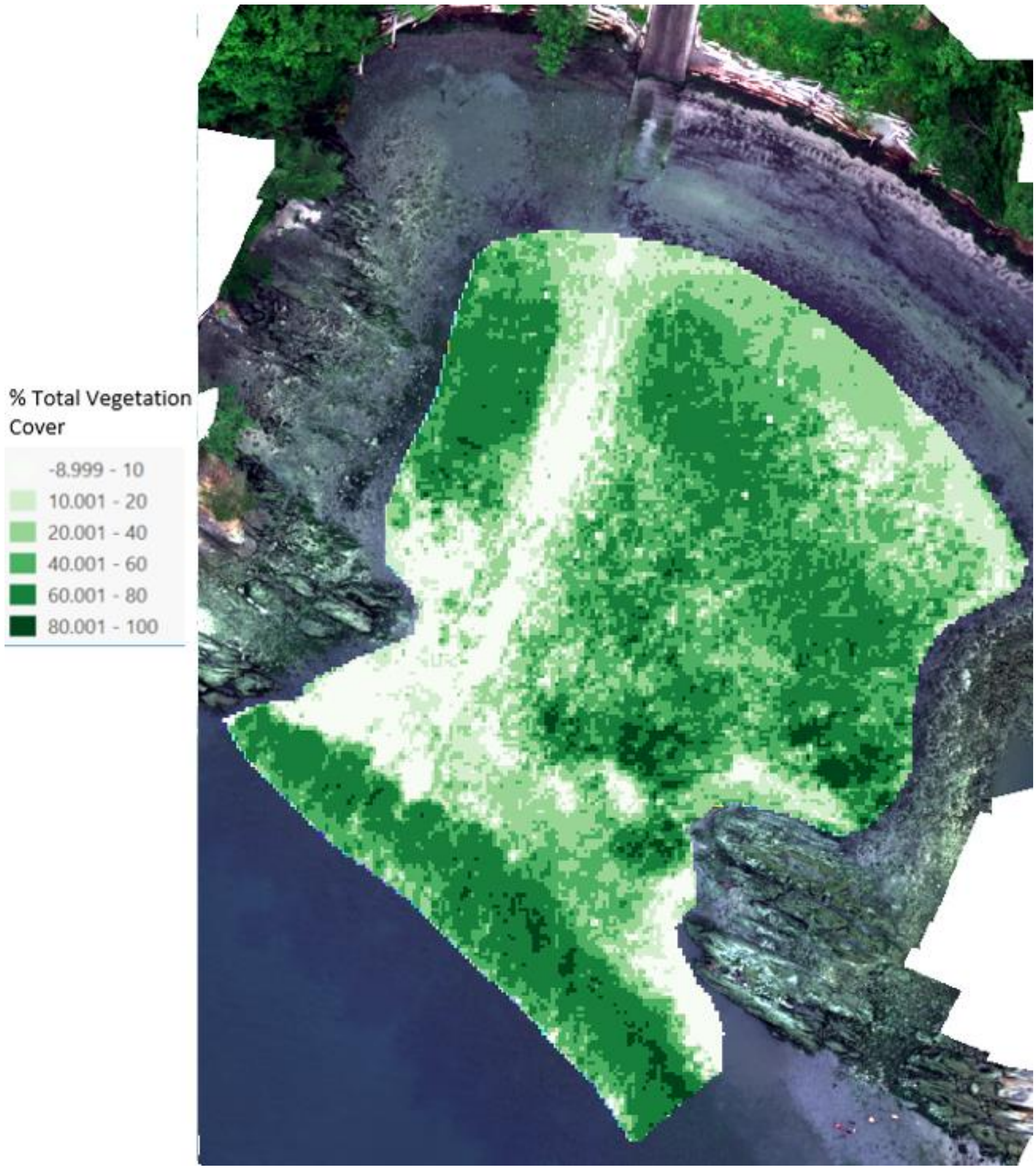

Figure 12: Percent total vegetation cover for the mudflat and subtidal eelgrass for August 28 using the NDI vegetation index and equation in Figure 7. Total vegetation cover includes both eelgrass and algae. Area outside the mudflat is the RGB image for this date to provide context relative to upland and the paved boat ramp.

By simply subtracting the vegetation cover layers for each date, I can quantify the change in vegetation cover. These results are presented in Figure 13-15.

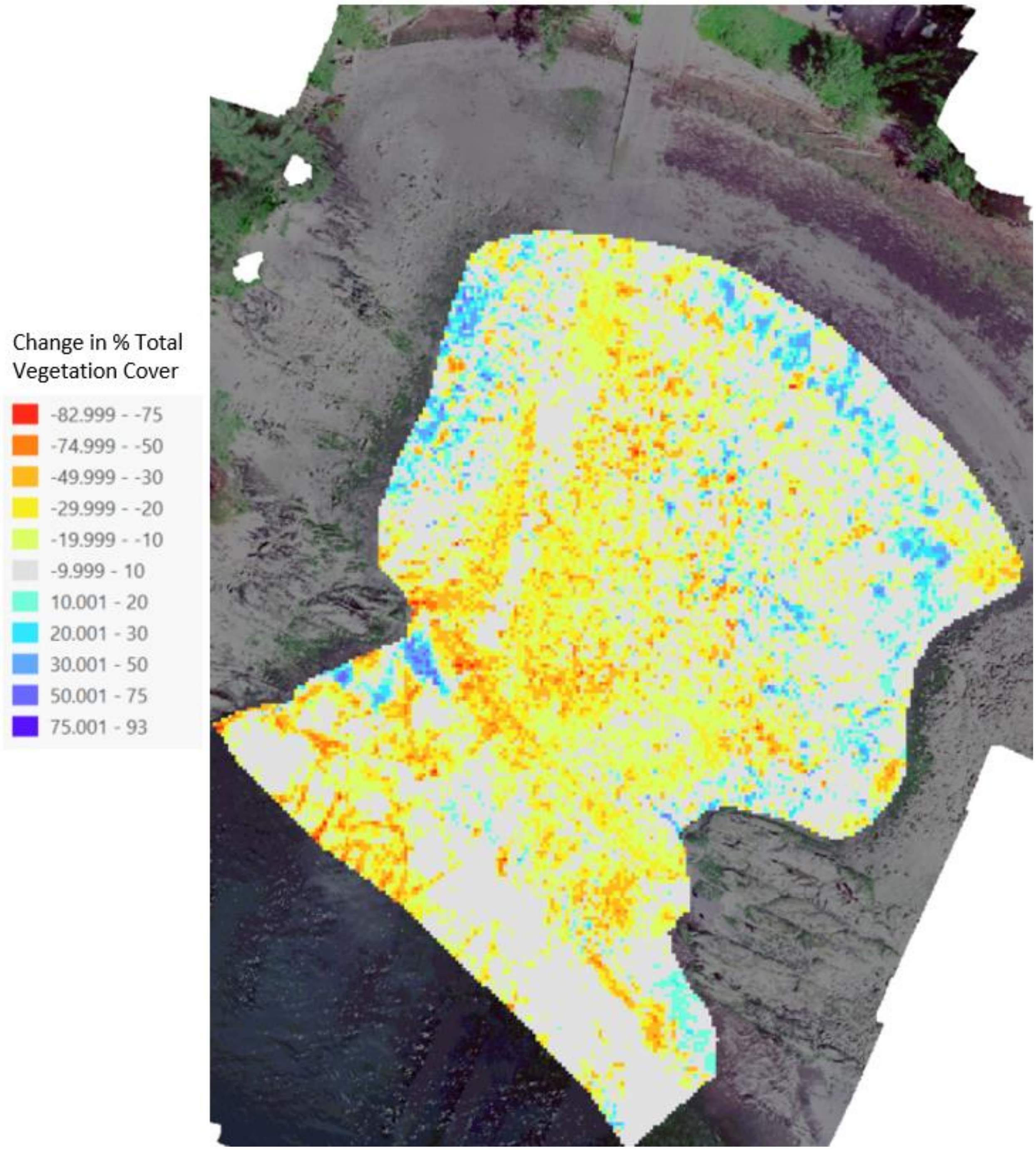

Figure 13: Change in total percent vegetation cover between July 14 and July 17. Negative values represent loss of vegetation cover and positive values represent increase in vegetation cover.

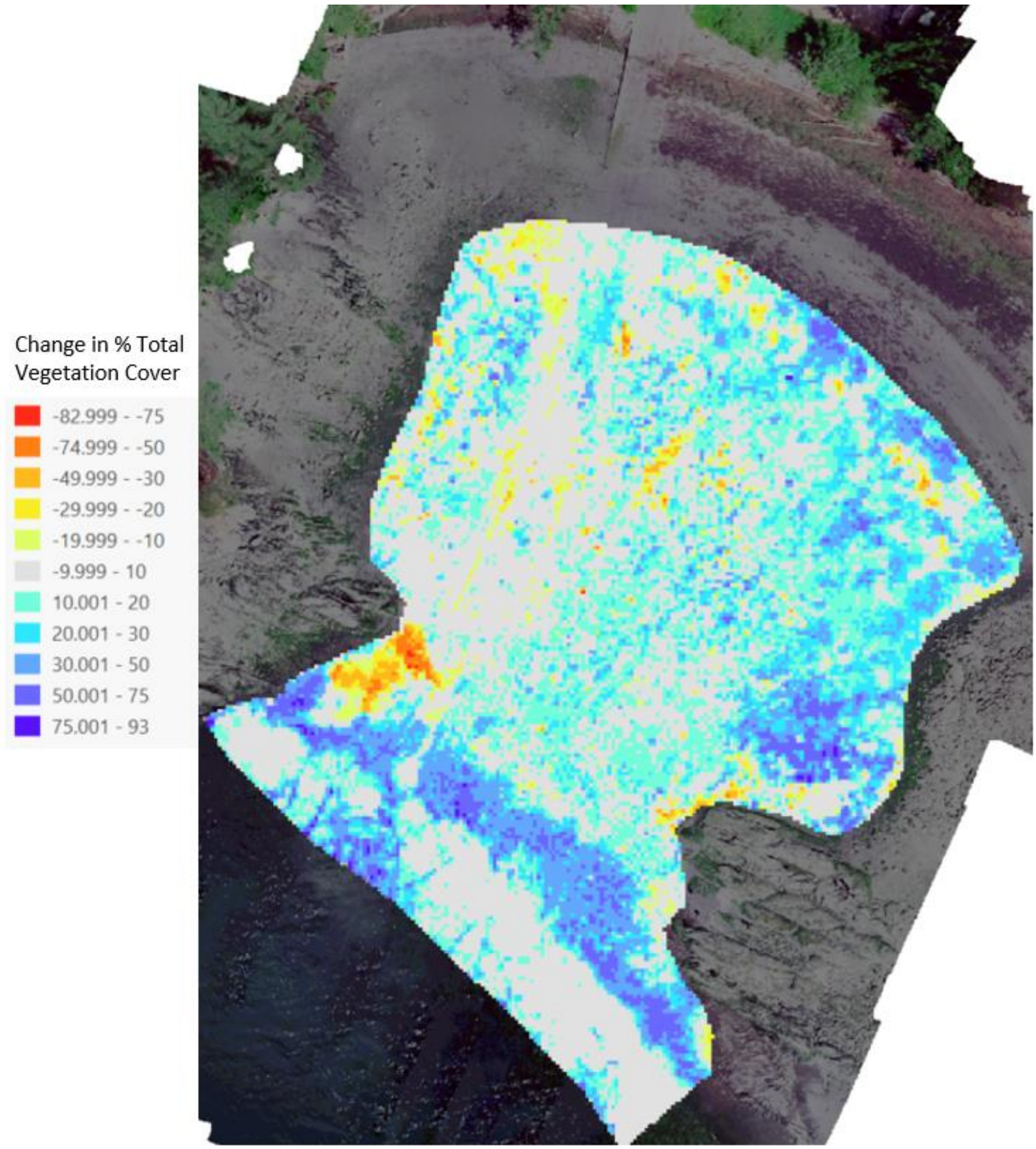

Figure 14: Percent change in total vegetation cover between July 17 and July 31. Negative values represent loss of vegetation cover and positive values represent increase in vegetation cover. Increase in vegetation cover here mostly reflect typical seasonal growth.

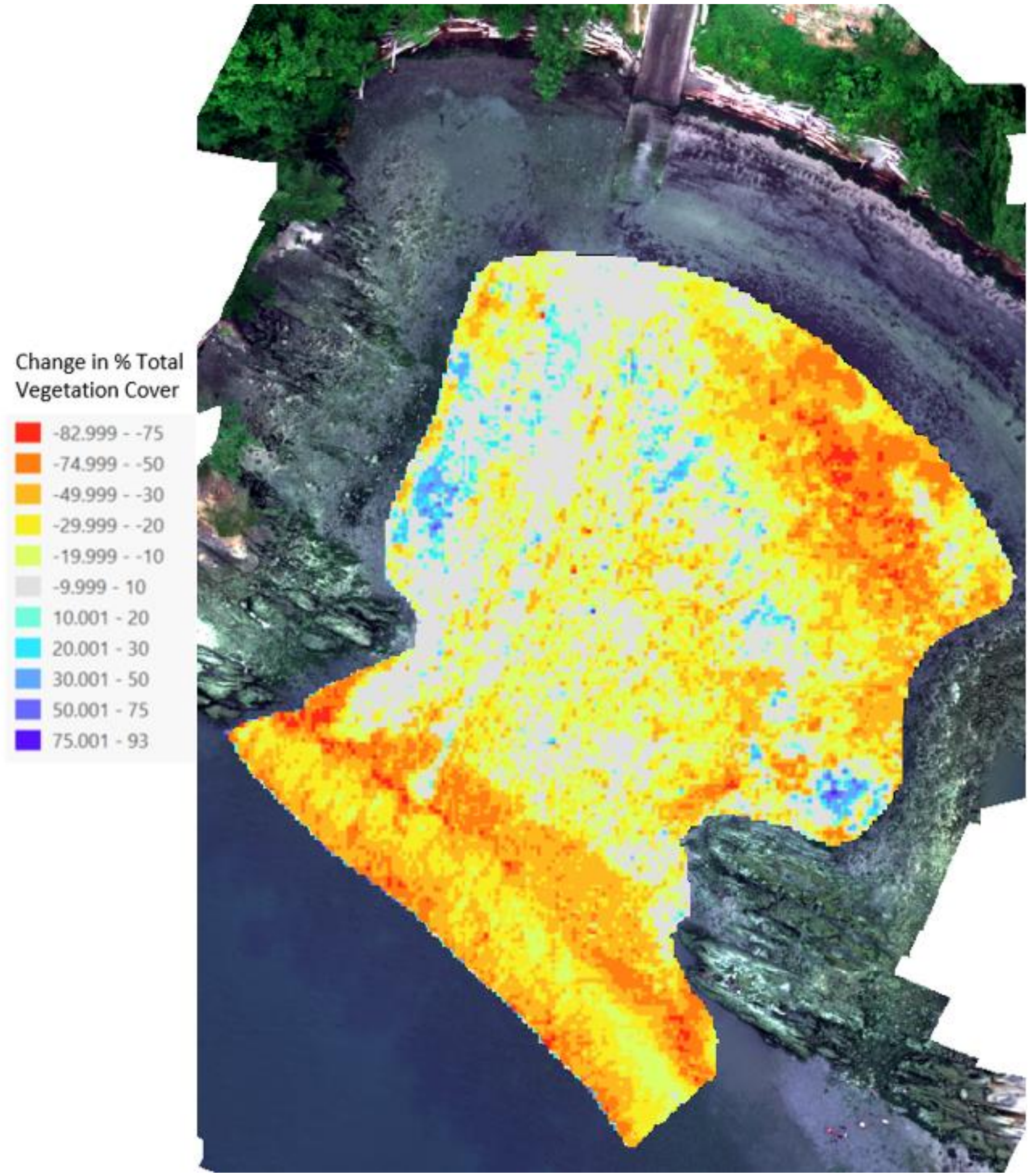

Figure 15: Percent change in total vegetation cover between July 31 and August 28. Negative values represent loss of vegetation cover and positive values represent increase in vegetation cover. Much of the decrease in vegetation cover reflects typical seasonal senescence.

Figure 13 indicates extensive loss of vegetation cover between July 14 and 17 on either side of the main path from the paved boat ramp to the water. Presumably this resulted from a busy weekend with multiple people driving across the mudflat to launch boats simultaneously and therefore fanning out across the mudflat. This trend continues between the 17th and the 31st but the impact is much reduced (Figure 14). The increases in vegetation cover away from this path results from the typical seasonal growth of both eelgrass and algae as they reach the peak of their biomass at roughly this time of year. There are additional reductions in vegetation cover along the boat launch track between July 31 and August 28 (Figure 15), however the extensive declines in vegetation cover throughout the cove are the result of typical season declines in both eelgrass and algae.

Conclusions

The objective of this analysis was to evaluate the impacts of boat launch activities in Wildcat Cove. The work is motivated by concerns over impacts on eelgrass. However, boat launch activity may have broader impacts on a variety of ecosystem services and on other organisms that occupy this habitat, including crabs, clams and salmon. My analysis focuses on variation in the coverage of both eelgrass and algae. With additional work, it would be possible to focus more narrowly on eelgrass alone. However, I feel that documenting the impacts of boat launch activity on both eelgrass and algae provides a broader assessment of environmental impacts

These results clearly indicate that boat launch activities in Wildcat Cove have an impact on the coverage of eelgrass and algae. The spatial extent of the impacts are primarily limited to an area that is roughly 20 x 90 m. On busy weekends, as multiple groups are launching boats, vehicles fan out across the mudflat and the width of the impacted area expands. On July 17, after the busy opening weekend of crabbing season, the main path through the mudflat was deeply rutted and a bit wider (Figures 3, 6b). In some cases, it is apparent that some vehicle swing out quite far from the main track either to avoid other vehicles or seeking a less rutted track (Figure 6 b,c,d). It is also apparent that the passage of boats through the subtidal eelgrass results in loss of eelgrass, presumably from boat propellers (Figures 9 and 10). By July 31, the impacted area has continued to expand and there are a few stray scars in the eelgrass well off to the side of the main track (Figures 4, 6c and 11). Late July is near the peak of the growing season for eelgrass and the track through the subtidal eelgrass appears to have regrown and mostly filled in (Figure 11). By August 28, there appears to be some expansion of impacts along the main launch track across the mudflat but this is difficult to evaluate since there is an obvious decline in vegetation cover throughout the cove that simply reflects typical seasonal declines.

Mitigation

Wildcat cove is an extremely popular boat launch and closing the site does not seem practical. One approach to reducing impacts might involve using a series of buoys or pilings, combined with an education effort, to restrict vehicle traffic across the mudflat to a single lane. This would prevent vehicles from fanning out across the mudflat and restrict the impacts to a much narrower corridor. This would create backups on busy weekends but this could have some advantages. In some cases, those launching kayaks and other small boats drive a vehicle across the mudflats to the water's edge. By restricting vehicles to a single lane, the backups would encourage kayakers to carry their boats to the water rather than driving across the mudflat. This would in turn reduce the number of vehicle trips across the mudflats at low tide. Restricting traffic to single lane could result in more churning of the mud in this single lane and it might be necessary to install a series of cement pads leading all the way to the water's edge to prevent vehicles from getting stuck. The addition of buoys, pilings and cement pads would require permits that would need to be negotiated with DNR.